Available online at www.sciencedirect.com
ScienceDirect
Computer-Aided Design 39 (2007) 229–244
COMPUTER-AIDED DESIGN
www.elsevier.com/locate/cad

Systematic geometric rigid body error identification of 5-axis milling machines

Erik L.J. Bohez[a,*], Bancha Ariyajunya[b], Chanin Sinlapeecheewa[c], Tin Maung Maung Shein[a], Do Tien Lap[d], Gustavo Belforte[e]

[a] *Asian Institute of Technology, P.O. Box 4, Klong Luang, Pathumthani 12120, Thailand*
[b] *Burapha University, 169 Long-Hard Bangsaen Road, Tambon Saensook, Amphur Muang, Chonburi 20131, Thailand*
[c] *Fabrinet Co. Ltd., 294 Moo 8 Vibhavadi-Rangsit Road Kukot, 12130 Lam Luk Ka, Pathumthani, Thailand*
[d] *Le Qui Don University, 100, Hoang Quoc Viet Street, Cau Giay District, Hanoi, Viet Nam*
[e] *Politecnico di Torino, Corso Duca degli Abruzzi 24, 10129 Torino, Italy*

Received 27 October 2005; accepted 29 November 2006

Abstract

A 5-axis milling machine has 39 independent geometric error components when the machine tool is considered as a set of five rigid bodies. The identification of the deterministic component of the systematic error is very important. It permits one to improve the accuracy close to the repeatability of the machine tool. This paper gives a new way to identify and compensate all the systematic angular errors separately and then use them further to identify the systematic translational error.

Identification based on a new mathematical method and a stable numerical solution method is proposed. The model explains from first principles why some error components have no effect in a first order model. The identification of the total angular systematic errors can be done independently from the translation errors. However, the total translation error depends on the angular errors and the translation errors of each machine tool slide. The main problems solved are to find enough linear independent equations and avoid numerical instability in the computation. It is important to separate numerical problems and linear dependence. The very complex equations are first analyzed in symbolic form to eliminate the linear dependencies. The total of linear independent components in the model is reduced from 30 to 26 for the position dependent errors and from 9 to 3 for the position independent components. Secondly, the large system of linear equations is broken down in many smaller systems. The model is tested first with simulated errors modeled as cubic polynomials. An artifact-based identification is proposed and implemented based on drilling holes in various locations and orientations. New ways to measure the volumetric error directly are proposed. Direct measurement of the total volumetric error requires considerably less measurement than measuring all 6 components of each machine slide especially in the case of a 5-axis machine.

Keywords: Systematic errors; Rigid body; 5-Axis machine tool; Error compensation; Inverse kinematics

1. Introduction

Machines with three linear axes have a total of 21 linear independent geometric error components [28]. These components can be identified and compensated for as can be seen in many research results. However, it should be clear that for a 3-axis machine these errors can be corrected only for a single contact point between the tool and workpiece or cutter contact (CC) point. The point selected for the correction is the CL (Cutter Location) point. The CL point is a convenient reference point on the tool such as the tool tip coordinates. An error that cannot be eliminated in a 3-axis machine tool is due to the angular errors in the vector connecting the CC to the CL point as discussed in [1]. The 5-axis machine gives us the possibility to compensate for these angular systematic errors by adjusting the rotational axes. A 5-axis milling machine has 39 independent geometric error components when the machine tool is considered as a set of rigid bodies. Each axis slide considered as a rigid body has 6 errors, one for each degree of freedom. The errors due to the non-orthogonality

* Corresponding address: Asian Institute of Technology, Department of Design and Manufacturing Engineering, 12120 Pathumthani, Thailand.
E-mail address: bohez@ait.ac.th (E.L.J. Bohez).

0010-4485/$ - see front matter © 2006 Elsevier Ltd. All rights reserved.
doi:10.1016/j.cad.2006.11.006

of the machine coordinate system or squareness errors have 7 independent components. There are two independent rotational axes position offset errors.

2. Literature review

Bohez [1] analyzed the systematic errors in the 5-axis tool path generation. An overall model and strategy to compensate these errors is outlined. It is suggested that identification of the errors can be done by direct measurement or by using suitable workpieces or artifacts.

Belforte et al. [2] develop a self-calibration model based on 18 independent error components for Coordinate Measuring Machines and 3-axis machine tools. Reduced order Legendre polynomials are used to model and identify these 18 functions. A new identification method is outlined. It is assumed that the parts of the errors that cannot be compensated by the model are unknown but bounded.

In a series of three papers Kirienda and Ferreira [3–5] model and identify the quasi-static systematic errors for 3-axis NC machines. The independent parameters can be modeled as an n-dimensional polynomial. A first order polynomial model is shown to contain 17 independent parameters to be identified. These parameters are identified by measuring the position of 27 rectangular posts in the machine tool workspace. This arrangement provides 3×27 measurements XYZ. From these given set of possible points the minimal numbers of points is determined in such a way as to minimize the coefficient matrix condition number. The unknown parameters are obtained by directly inverting the coefficient matrix of the linear system. The least-squares approach is considered too slow. The best sample points are found to be on the borders of the rectangular workspace. These results could also be obtained without minimizing the condition number as the optimal sampling of a linear line segment is at the segment limits. The presented method is however more efficient when second order or higher polynomials are used to model the errors. Another important conclusion is that the linear order model seems to be an adequate model for a real machining center.

Tajbakhsh et al. [6] extend the model of Kirienda and Ferreira [3–5] by minimizing the $L\infty$ norm for three-axis machining centers. This norm minimizes the maximum error instead of minimizing the average square error. This is obtained by using linear Chebyshev polynomials.

Soons et al. [7] present a general model for multi-axis machines including 5-axis NC machines. They model the direct kinematics of the workpiece and tool kinematics chain. The errors are modeled as piecewise polynomials. They claim to obtain adequate models for 4 pieces of quadratic polynomials. It is suggested that piecewise linear functions should also be sufficient. The unknown parameters are estimated by the least squares method. They find the best sampling points by selecting those points out of a fixed regular grid of gauge blocks that minimize the covariance matrix by an iterative process. The relation between the number of parameters that can be estimated with the model and the machine axes is not discussed.

Srivastava et al. [8] model the geometric errors of a 5-axis machine as linear functions and the thermal errors as exponential variations with time of the parameters of these linear geometric errors with time. They use the direct kinematics homogenous matrix transforms. They observe that the rotational errors are independent of the translational errors. They also observe that the errors cannot be fully compensated. One of the rotational errors cannot be compensated with their model. They claim that this is due to the fact that the machine has only 5 degrees of freedom. It is also pointed out that this problem could affect the accuracy of swarf or flank milling in 5-axis mode.

Florussen et al. [9] identify the geometric errors in a 5-axis machining center based on a ball bar based length measurement. They start by using the reduced 21 independent parameter model for a 3 linear axis machine. The two rotational degrees are ignored to simplify the model. They claim that the error in the orientation can only be fully compensated with three rotational axes. They further reduce the number of 21 independent parameters by investigating the correlation between them. The rotational error components are found to be highly correlated with the corresponding straightness error components for the specific 5-axis machine (Maho 700s). These results are used to justify the removal of the 6 straightness errors from the 21-parameter model. They further reduce the number of parameters to 12 by observing that the linear error in the X, Y and Z directions is strongly correlated with the corresponding rotational errors. They further investigated the effect of the order of the polynomials used to model the errors. It is found that a quadratic or linear polynomial is sufficient for each error component in the reduced parameter model. The laser interferometer confirms that the linear and rotational errors are close to linear polynomials. The merit of above approach is great simplification of the calibration process. The correlation between components that are supposed to be linear independent was not explained.

Lin and Shen [10] propose the matrix summation approach to simplify the homogenous matrix transform approach. Their approach is based on a first order model and provides a clearer physical interpretation.

Ramesh et al. [11,12] analyze the effect of the temperature of critical building blocks on the machine tool errors. They point out that even with the same temperature distribution, there is also a large effect due to different machine tool operating parameters such as material removal rate, cutting parameters, wet or dry cutting, etc. The experimental data is classified using a Bayesian network with a rule based system.

Bagshaw and Newman [13] point out that the total errors in the workpiece are not only due to the machine inaccuracy but are also due to the fixture and programming errors. They develop an expert system that provides for rapid diagnosis and elimination of errors.

Bjorklund et al. [14] compensate errors that are due to tool path generation for 5-axis high-speed machining. The errors considered are mainly servo lag errors which are compensated by a fuzzy logic expert system active in the postprocessor.

Wang et al. [15] propose an error compensation model based on a meshed workspace where the errors are known at the nodes of the mesh. Once the errors are know for the mesh points the algorithm interpolates to find the errors in the whole workspace.

Jha and Kumar [16] present a scheme to compensate the geometric errors and analyze the effect on the accuracy of a cam profile.

Lei and Hsu [17] develop a probe-ball device that can be considered as a single side non-extensible double ball bar. The ball joint is fixed at the end of a standard measuring probe. Because of the fixed length and single ball joint, the motion is limited to paths on a sphere. Because of the geometric errors the probe will measure the small variations in the length that are then used to find the errors.

Lei and Hsu [18] classify the 5-axis CNC errors in motional errors due to inaccurate motion servo controls and link errors due to mounting errors of the machine structural components. The link errors of the rotary tables are normally not measurable due to limited accessibility. They use their direct measurement method developed in [17] combined with least square identification for the link errors of the rotary axes. They use the total differentials of direct and inverse kinematics relation between the workpiece and machine coordinates to implement real-time error compensations as suggested in Bohez [1].

Chen et al. [19] develop a new error identification and accuracy improvement model. They use a meshing concept to subdivide the workspace into smaller 3D elements. A suitable interpolation scheme allows them to find the errors at any location in the workspace.

Mou and Lui [20,21] develop an on-machine inspection method based on measuring a reference part on the machine tool to identify and compensate the quasi static error. They compare quadratic and cubic polynomials for the errors. Better results are obtained with a cubic model. They also look at the variation of the errors due to the temperature.

Abbaszadeh-Mir et al. [22] classify the rigid body geometric errors in two groups. The first group is the position independent geometric errors also called link errors such as misalignments, angular offsets and position distance between rotary axes. The second group is the position dependent geometric error parameters that vary with the position of the machine slides. They identifying the total number of position independent geometric errors as eight. Kinematic considerations give the formula $n = 4r + 2p + 6 = 20$ for the total number of position independent geometric error (r = # rotational axes, p = # translational axes). However, from these 20 only 8 are linearly independent. They use the rank, singular value decomposition and the condition number of the Jacobian to single out these independent error parameters. They then propose to use a telescoping magnetic ball bar based algorithm to identify these 8 errors.

Mahbubur et al. [23] improve the positioning accuracy in 5-axis milling by identifying the angular error. They use a ball bar to identify this error. The results are then used in the postprocessor by taking these orientation errors into account in the inverse kinematics.

Tsutsumi and Saito [24] identify the geometric errors related to the two rotary axes of a 5-axis machine. They consider the angular deviations of the rotary axes, including the positional deviations. Specifically they identify 8 deviations. These are the three angular and three positional errors of the A-axis relative to the machine coordinate system. The other two deviations are the angular error and distance errors between the two rotary axes. They use a ball bar to identify these errors considered constant.

Lee and Ferreira [25,26] introduce a new method based on triangulation for 2D and tretragonalization for 3D with linear transducers. They introduce redundant measurements in the procedure. This redundancy together with the concept of transistivity allows for the use of inaccurate transducers. This method is applied to 2 and 3 linear axis machine tools.

Remus and Feng [27] give a generic kinematic model for 5-axis machine tools applicable to all 5-axis machine configurations. They illustrate the versatility of the generic model to evaluate the kinematic performance of the possible designs of the two rotational joints. The optimal distance and orientation of the rotational axes is investigated.

Kruth et al. [29] use a ball plate artifact to identify the 21 error components of a 3 linear axis CMM machine. The 3 squareness errors are not modeled but included in the first degree part of the translational errors. The errors are modeled as cubic Legendre polynomials. To identify all the coefficients of the polynomials, 22 overlapping positions parallel to the XY, XZ and YZ planes and 4 positions at an arbitrary position are needed. They need to use only 10 out of the 16 balls for each position. The size of the ball plate is limited by practical considerations and time. A large ball plate requires fewer measurements but will be more difficult to handle.

From the literature it can be concluded that researchers reduce the number of parameters without clearly justifying it based on first principles. The reason to reduce the parameters is however clear. The more parameters there are the more numerical problems. This is the same for the degree and type of the polynomials. The methods used can be classified in direct measurement on the machine and offline or online measurement of an artifact or reference part. The direct measurement methods are today often based on a laser interferometer placed outside the machine or on the machine table, or a ball bar. The interferometer has the potential to determine all 39 components directly in the case of a 5-axis machine tool. However the rotation errors of the machine slide around the laser beam axis are difficult to identify. Also it is difficult to identify the error components for the rotary axes.

Commercial artifact based systems are commonly based on a ball plate or hole plate and a measuring probe placed in the machine spindle. A considerable part of the cost of these systems is due to the black box type software. Most of these are only for 3-axis machine tools and CMM machine calibration. Table 1 shows that the researchers that tried to tackle the problem of error identification in 5-axis machine tools always made simplifications in the final number of parameters that were not justified on first principles. The basic reason or method for reducing the number of parameters is given in the last column of this table.

Table 1
Relevant 5-axis machine tool error identification research papers comparison

Paper ref	Lin	Rot	Sqr	# Par	Method	Deg	Experiment	Parameter reduction
[1] [*] Bohez	17	15	7	39/32	LSQ	3	Sim/holes	Linearly dependent, 1st order
[7] Soons	15	15	0	f(typ)	LSQ	2	Rectangular grid	Cost/until easy to solve
[8] Srivastava	15	15	0	30	Direct	1	Sim	Low degree
[9] Florussen	9	3	0	12	LSQ	2	Sim/laser	Correlated parameters
[10] Lin	15	15	7	37	na	na	None	Not attempted to solve
[18,17] Lei	34	21	7	61/59/13	LSQ	0	Laser/probe ball	Only not measurable errors
[22] Abbaszadeh	21	21	0	42/20/8	Direct	0	Sim/ball bar	Matrix rank
[23] Mahbubur	4	4	0	8	Direct	0	Ball bar	For 2 rotary axes only
[24] Tsutsumi	5	8	0	8	Direct	0	Ball bar	For 2 rotary axes only

Lin: Number of linear error components; Rot: Rotational error components; Sqr: Squareness error components; # Par: Number of independent parameters in the model (e.g. 61/59/13 means that the model starts with 61 independent parameters that are then further reduced to 59 and finally to 13 for which the model is solved; f(typ) refers to reduction based on the type of machine and other very machine specific information not clearly justified); Method: Method by which the linear systems is solved (e.g. LSQ: Least Square Method, direct: direct inversion of coefficient matrix, na: not attempted to solve); Deg: Refers to the degree of the polynomial used for the identification for the errors that vary with machine slide position; Experiment: Experiments done (e.g. sim: simulation, holes: drilling holes, laser: laser interferometer); Parameter reduction: Gives the method used by the researcher to reduce the number of parameters.

In the rest of this paper [*] the total number of linear independent parameters is obtained from first principles as is discussed in the following sections.

3. Mathematical model

3.1. Degrees of freedom and independent error components

A rigid solid body has 6 degrees of freedom [30]. The 6 coordinates uniquely specify the position of a rigid body in 3D space. A 5-axis machine has 5 slides that can move relative to each other. Two other bodies that are fixed to the machine are the tool and the workpiece. Each body M has 6 independent errors T_{MX}, T_{MY}, T_{MZ}, R_{MX}, R_{MY}, and R_{MZ}. In the previous notation T means translational, R means rotational. The rotational errors are often referred to as pitch, roll and yaw. The first subscript M stands for the name of the concerned rigid body. The letter M will take following names: X, Y, Z, A, B or C representing each machine slide of the 5-axis machine tool. The second subscript designates the axis of translation for a T error and the axis of rotation for an R error.

The total number of errors is $6 \times 7 = 42$ errors due to the positions of 7 rigid bodies relative to a coordinate system fixed to the laboratory. These 7 bodies move relative to each other. There can still be errors due to the position of 7 the fixed coordinate systems to each rigid body. The number of independent error components due to these can be found by connecting these 7 rigid bodies by the minimum number of rigid bars to form a single rigid body. Three rigid bodies can be connected by 3 rigid bars in a rigid triangle. Four bodies require 6 rigid bars (tetrahedron). Seven bodies will require 15 rigid bars. For n bodies the formula $3(n-2)$ can be used. The total of independent error components for 7 rigid bodies is $(42 + 15) = 57$. The error components due to the workpiece and the tool are not considered in the model. These errors are random in nature in the sense that they are different for each new set up. However, the above determination of the error components shows clearly that these errors are there and should be as small as possible by careful positioning of the tool and workpiece. These requirements are clearly favoring the tool and workpiece offset measurement on the machine through in process measurement.

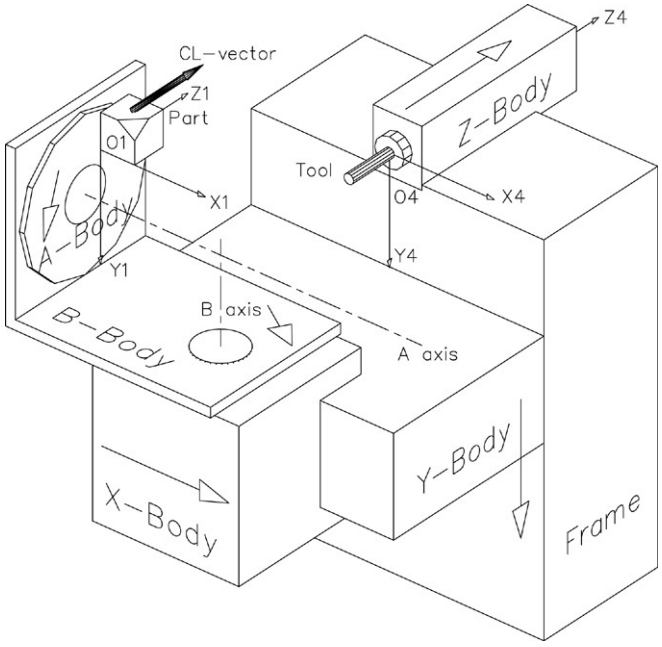

Fig. 1. Maho 600E 5-axis machine.

In our model only 5 rigid bodies are considered. There will thus be $30 + 9 = 39$ independent errors. The Figs. 1 and 2 shows the 5-axis machine and the corresponding kinematic link diagram of the same machine that will be considered in our research. Fig. 1 shows the workpiece coordinate system $O1$ with the Cutter Location vector (CL). The motion of the machine should be such that this CL vector coincides with the tool. The difference between the CL vector and tool is the total closed loop volumetric error [1] $\mathrm{d}X, \mathrm{d}Y, \mathrm{d}Z$ and $\mathrm{d}i, \mathrm{d}j, \mathrm{d}k$. This concept is very useful to assess the effect of each individual error component.

3.2. Reference coordinate system and squareness error

The machine has one position that is defined as the reference position. Any convenient set can be chosen. One reference

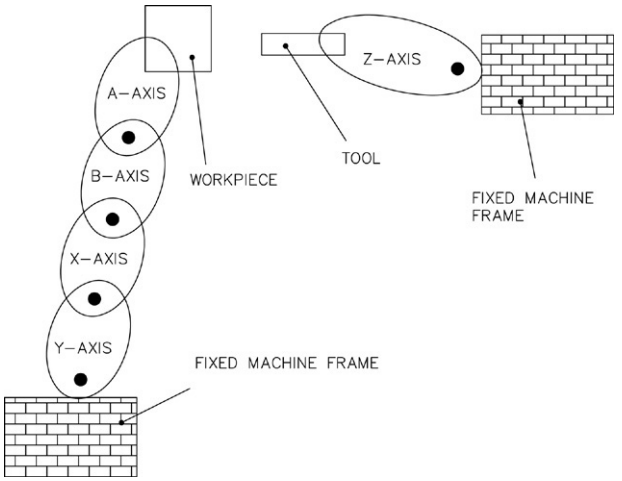

Fig. 2. Kinematic link diagram of Maho 600E 5-axis machine.

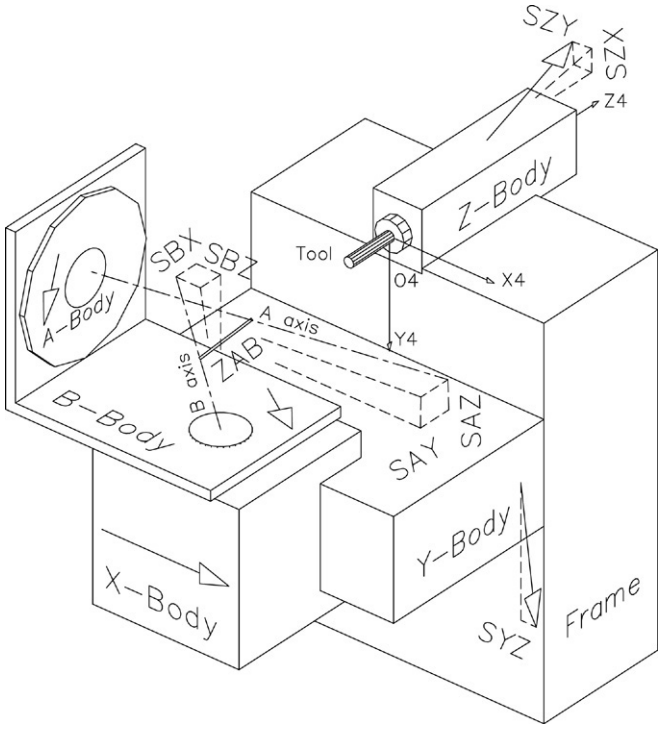

Fig. 3. Squareness errors S_{YZ}, S_{ZX}, S_{ZY}, S_{AY}, S_{AZ}, S_{BX}, S_{BZ} and eccentricity Z_{AB}.

coordinate systems is fixed to the machine frame and to each body in the kinematic chain. For the reference Cartesian coordinate systems, all the X-reference axes coincide with the real X machine axis. So the real X axis has no angular error or squareness error component. The plane through real X and real Y axis of the machine tool is selected as reference plane. So the real Y axis can have only one angular or squareness error S_{YZ}. The real Z axis will have two squareness errors S_{ZX} and S_{ZY}. These squareness errors are shown in Fig. 3.

The squareness error [28] is due to the error in the direction of the real axes of the machine. For example the A-axis is not exactly parallel with the X-axis reference. The A-axis will have 2 squareness errors S_{AY} and S_{AZ}. The same is valid for the

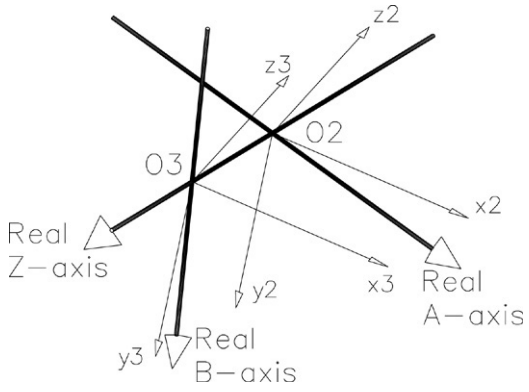

Fig. 4. Offset error $r_{AB} \approx z_{AB}$ between A and B rotary axes for machine in Fig. 1.

other rotational axes B or C. The squareness errors of the 5-axis machine in Fig. 1 will be:

X-axis: none because the real X axis coincides with the reference X-axis

Y-axis: S_{YZ}

Z-axis: errors S_{ZX} and S_{ZY}.

A-axis: S_{AY} and S_{AZ}.

B-axis: S_{BX} and S_{BZ}.

These 7 squareness error are constant angles independent of the machine slide coordinates, or in other words the position.

3.3. Rigid body errors

When the machine slides move relative to the reference coordinate system small angular and linear errors will add to the nominal translations and rotations.

A local reference coordinate system is fixed to each body and coincides with the reference coordinate system fixed to the machine frame. Moving the machine slides will give 3 small translations and 3 small rotations due to the systematic errors. Only 4 reference coordinate systems need to be considered. The workpiece reference coordinate system $O1$ is fixed to the rotary table A and the workpiece. The reference coordinate system $O2$ is fixed to the rotary table B. The $O3$ system is fixed to the Y slide body. When the machine is in the reference position all this reference coordinate systems orientations coincide and the machine controller displays zero for each axis.

The origins $O2$ and $O3$ are not at the same location. There is a distance r_{AB} that gives the position error between the two rotational axes A and B. This offset is in the plane of intersection of the real Z-axis and real A-axis. This plane is unique and contains r_{AB} Therefore r_{AB} has only two independent components as illustrated in the Fig. 4. Only the offset in the Z direction Z_{AB} is of first order effect. Fig. 4 also illustrates how the reference position is set. The real Z-axis corresponds to the centerline of the spindle or tool centerline. It is possible to make the real A-axis centerline intersect with the real Z-axis by means of the Y translation. This gives the point $O2$. This intersection defines a plane. This plane is intersected by the centerline of the B rotation in the point $O3$. Because of the X translation it is possible to make the real B-axis

intersect with the real Z-axis. In $O2$ a reference coordinate system fixed to the B-body is introduced. In $O3$ a reference coordinate system fixed to the Y-body is introduced. Finally the coordinate system $O1$ is relocated at $O2$ to remove the workpiece offsets from the equations. $O4$ is relocated at $O3$. The tooltip is supposed to coincide with $O4$. This removes the tool offsets from our equations. This is a convenient way to eliminate all redundant offsets between the required coordinate systems.

3.4. Errors due to misalignment of rotary axis

Due to the squareness error of the rotational axis the first order model for a rotation A around the A-axis with squareness errors S_{AY} and S_{AZ} is given by:

$$\begin{aligned} X(A) &= X + YS_{AZ} - ZS_{AY} - YS_{AZ}\cos[A] \\ &\quad + ZS_{AZ}\sin[A] + YS_{AY}\sin[A] + ZS_{AY}\cos[A] \\ Y(A) &= Y\cos[A] - Z\sin[A] - XS_{AZ}\cos[A] \\ &\quad + XS_{AY}\sin[A] + XS_{AY} \\ Z(A) &= Y\sin[A] + Z\cos[A] - XS_{AZ}\sin[A] \\ &\quad - XS_{AY}\cos[A] + XS_{AZ}. \end{aligned} \tag{1}$$

The above equations are obtained by rotating the point X, Y, Z over an angle A around the axis A in the coordinate system $O2$. Whenever there are products of the S_{AZ} and S_{AY} the terms are neglected.

The same equations can be derived for a B-axis or C-axis.

3.5. First order model of errors

It is assumed naturally that the tool has been aligned with the real Z-axis of the machine. Due to the squareness errors and the Z-axis body there will be errors in the tooltip coordinate as follows (Z is the translation of the real machine tool Z axis):

The tooltip coordinate after the translation Z relative to the reference coordinate system $O4$ will be:

$$\begin{aligned} X_{4t} &= S_{ZY}(Ztip + Z) + R_{ZY}(Ztip + Z) + T_{ZX}; \\ Y_{4t} &= -S_{ZX}(Ztip + Z) - R_{ZX}(Ztip + Z) + T_{ZY}; \\ Z_{4t} &= Ztip + Z + T_{ZZ}; \end{aligned} \tag{2}$$

$Ztip$ is the coordinate of the tool tip.

It can already be observed that the component R_{ZZ} has only second order effect and will not appear in the first order model.

The workpiece will rotate over angles A and B and will translate a distance X and Y along the real axes of the machine (see Figs. 1 and 2).

The final position (first order) of the workpiece coordinate X_{4w}, Y_{4w} and Z_{4w} in the machine reference system $O4$ will be given by three equations each consisting of many terms and too long to write down here. The error in the position will be the difference between the tool tip coordinates and the workpiece coordinates. The error terms and the corresponding coefficients are given in Tables 2–4.

This position errors can also be expressed in the workpiece coordinate system rigidly fixed to the workpiece by applying the inverse of the rotations B and A to the position errors $\mathrm{d}X$, $\mathrm{d}Y$, $\mathrm{d}Z$.

These errors could be measured for example by a laser interferometer as a function of different machine translations X, Y, Z, A and B. If the interferometer is fixed to the machine frame the equations in Tables 2–4 have to be used. If the interferometer is fixed to the machine table instead the equations in Tables 2–4 must first be transformed to the workpiece coordinate system. This last method is often not practical for direct measurement with an interferometer. However if the errors are obtained from a reference workpiece or artifact the equations in Tables 2–4 must also be transformed to the workpiece coordinate system.

Table 2
The error terms and coefficients of $\mathrm{d}X$ in workpiece coordinates

Error component	Coefficient
$T_{BX} + T_{XX} + T_{YX} - T_{ZX}$	1
$R_{BZ} + R_{XZ} + R_{YZ} + S_{BZ} - S_{YZ}$	Y
$R_{AY} + R_{BY} + R_{XY} + R_{YY} - R_{ZY} + S_{AY} - S_{ZY}$	Z
S_{AY}	$-Z\cos[A]$
S_{AZ}	$-Y\cos[A]\cos[B]$
S_{AZ}	$Z\sin[A]$
T_{AX}	$\cos[B]$
$R_{AZ} + S_{AZ} - S_{BZ}$	$Y\cos[B]$
S_{AY}	$-Y\sin[A]\cos[B]$
T_{AZ}	$\sin[B]$
$S_{BX} - R_{AX}$	$Y\sin[B]$

Table 3
The error terms and coefficients of $\mathrm{d}Y$ in workpiece coordinates

Error component	Coefficient
$T_{AY} + T_{BY} + T_{XY} + T_{YY} - T_{ZY}$	1
$R_{BZ} + R_{XZ} + S_{BZ}$	$-X$
$-R_{BX} - R_{XX} - R_{YX} + R_{ZX} - S_{BX} + S_{ZX}$	Z
$-R_{AZ} - S_{AZ} + S_{BZ}$	$X\cos[B]$
$-R_{AX} + S_{BX}$	$Z\cos[B]$
S_{AZ}	$X\cos[B]\cos[A]$
S_{AY}	$X\cos[B]\sin[A]$
$R_{AX} - S_{BX}$	$X\sin[B]$
$-R_{AZ} - S_{AZ} + S_{BZ}$	$Z\sin[B]$
S_{AZ}	$Z\cos[A]\sin[B]$
S_{AY}	$Z\sin[B]\sin[A]$

Table 4
The error terms and coefficients of $\mathrm{d}Z$ in workpiece coordinates

Error component	Coefficient
$T_{BZ} + T_{XZ} + T_{YZ} - T_{ZZ}$	1
$R_{AY} + R_{BY} + R_{XY} + S_{AY}$	X
$+R_{BX} + R_{XX} + R_{YX} + S_{BX}$	$-Y$
T_{AZ}	$\cos[B]$
$-R_{AX} + S_{BX}$	$Y\cos[B]$
S_{AZ}	$X\sin[A]$
T_{AX}	$-\sin[B]$
$-R_{AZ} - S_{AZ} + S_{BZ}$	$Y\sin[B]$
S_{AY}	$Y\sin[A]\sin[B]$
S_{AY}	$-X\cos[A]$
S_{AZ}	$Y\cos[A]\sin[B]$

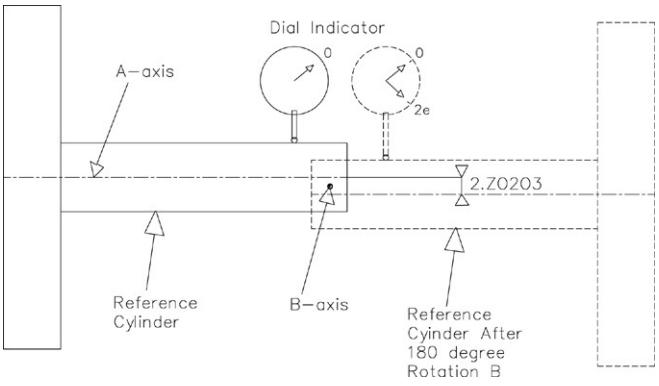

Fig. 5. Measurement of $zo2o3$.

Careful observation of the tables shows that some error terms have coefficients zero. This means that they have no influence on the corresponding error. Also it can be observed that there are rotational errors and squareness errors in the terms. If all the error terms are equal to zero the relation between the CL vector $X1, Y1, Z1, i1, j1, k1$ in the coordinate system $O1$ and the machine motions X, Y, Z, A and B are as follows:

$$\begin{aligned}
X &= -(X1\cos[B] + Xo1o2\cos[B] + Xo2o3\cos[B] \\
&\quad + Zo2o3\sin[B] + Z1\cos[A]\sin[B] \\
&\quad + Zo1o2\cos[A]\sin[B] \\
&\quad + Y1\sin[A]\sin[B] + Yo1o2\sin[A]\sin[B]) \\
Y &= -(Y1\cos[A] + Yo1o2\cos[A] \\
&\quad - Z1\sin[A] - Zo1o2\sin[A]) \qquad (3) \\
Z &= Zo3o4 - Ztip + Zo2o3\cos[B] + Z1\cos[A]\cos[B] \\
&\quad + Zo1o2\cos[A]\cos[B] + Y1\cos[B]\sin[A] \\
&\quad + Yo1o2\cos[B]\sin[A] - X1\sin[B] \\
&\quad - Xo1o2\sin[B] - Xo2o3\sin[B] \\
i &= -\sin[B]; \quad j = \sin[A]\cos[B]; \quad k = \cos[A]\cos[B].
\end{aligned}$$

The workpiece offsets or the coordinates of $O1$ in $O2$, $Xo1o2, Yo1o2, Zo1o2$ will be zero because $O1$ will coincide with $O2$. The coordinates of $O2$ in $O3$, $Xo2o3 = r_{AB}S_{ZY}$ and $Yo2o3 = r_{AB}S_{ZX}$, will be second order distances and $Zo2o3 \approx r_{AB}$. This $Zo2o3$ in the case of our machine was measured directly and is -0.080 mm. This value can be measured in a very simple way by putting a reference cylinder on the centerline of the A-axis with the machine in the reference position. A dial indicator is placed in the spindle and put on zero in contact with the cylinder. The B-axis is afterwards rotated 180°. The dial indicator will now give double the value of $Zo2o3$ (see Fig. 5).

The equations given in Tables 2–4 are given below for reference:

$$\begin{aligned}
\mathrm{d}X &= T_{BX} + T_{XX} + T_{YX} - T_{ZX} + R_{BZ}Y + R_{XZ}Y + R_{YZ}Y \\
&\quad + S_{BZ}Y - S_{YZ}Y + R_{AY}Z + R_{BY}ZR_{XY}Z + R_{YY}Z \\
&\quad - R_{ZY}Z + S_{AY}Z - S_{ZY}Z - \cos[A](S_{AY}Z \\
&\quad + S_{AZ}Y\cos[B]) + S_{AZ}Z\sin[A] + \cos[B](T_{AX} \\
&\quad + (R_{AZ} + S_{AZ} - S_{BZ})Y - S_{AY}Y\sin[A]) \\
&\quad + T_{AZ}\sin[B] - R_{AX}Y\sin[B] + S_{BX}Y\sin[B] \qquad (4)
\end{aligned}$$

Table 5
Orientation error di in machine coordinates

Error di in machine coordinates	Coefficient
$R_{AY} + R_{BY} + R_{XY} + R_{YY} - R_{ZY} + S_{AY} - S_{ZY}$	1
S_{AY}	$-\cos[A]$
S_{AZ}	$\sin[A]$

Table 6
Orientation error dj in machine coordinates

Error dj in machine coordinates	Coefficient
$-R_{BX} - R_{XX} - R_{YX} + R_{ZX} - S_{BX} + S_{ZX}$	1
$S_{BX} - R_{AX}$	$\cos[B]$
$S_{BZ} - R_{AZ} - S_{AZ}$	$\sin[B]$
S_{AZ}	$\cos[A]\sin[B]$
S_{AY}	$\sin[A]\sin[B]$

$$\begin{aligned}
\mathrm{d}Y &= T_{AY} + T_{BY} + T_{XY} + T_{YY} - T_{ZY} - R_{BZ}X - R_{XZ}X \\
&\quad - S_{BZ}X - R_{BX}Z - R_{XX}Z - R_{YX}Z + R_{ZX}Z - S_{BX}Z \\
&\quad + S_{ZX}Z + \cos[B](-R_{AZ}X - S_{AZ}X + S_{BZ}X - R_{AX}Z \\
&\quad + S_{BX}Z + S_{AZ}X\cos[A] + S_{AY}X\sin[A]) \\
&\quad + (R_{AX}X - S_{BX}X - R_{AZ}Z - S_{AZ}Z + S_{BZ}Z \\
&\quad + S_{AZ}Z\cos[A] + S_{AY}Z\sin[A])\sin[B] \qquad (5) \\
\mathrm{d}Z &= T_{BZ} + T_{XZ} + T_{YZ} - T_{ZZ} + R_{AY}X + R_{BY}X \\
&\quad + R_{XY}X + S_{AY}X - R_{BX}Y - R_{XX}Y - R_{YX}Y - S_{BX}Y \\
&\quad + (T_{AZ} - R_{AX}Y + S_{BX}Y)\cos[B] + S_{AZ}X\sin[A] \\
&\quad - T_{AX}\sin[B] - R_{AZ}Y\sin[B] - S_{AZ}Y\sin[B] \\
&\quad + S_{BZ}Y\sin[B] + S_{AY}Y\sin[A]\sin[B] \\
&\quad + \cos[A](-S_{AY}X + S_{AZ}Y\sin[B]). \qquad (6)
\end{aligned}$$

3.6. First order model of errors in the orientation

Eq. (3) clearly show that the tool vector components are only depending on the rotations A and B. This is not only the case for the 5-axis machine tool here (Fig. 1), it has been observed by others also [8,18,23] for other machine types.

The tool unit vector components after the translation Z relative to the reference coordinate system $O4$ will be (first order):

$$\begin{aligned}
i_{4t} &= S_{ZY} + R_{ZY} \\
j_{4t} &= -S_{ZX} - R_{ZX} \qquad (7) \\
k_{4t} &= 1.
\end{aligned}$$

The workpiece will rotate over angles A and B and will translate a distance X and Y along the real axis of the machine.

The final orientation of the cutter location vector i_{4w}, j_{4w} and k_{4w} in the machine reference system $O4$ will be given by three equations each consisting of many terms and too long to write down here. The error in the orientation will be the difference between the tool vector i_{4t}, j_{4t} and k_{4t} and the vector i_{4w}, j_{4w} and k_{4w}. The first order model is obtained by dropping all higher order terms. The first order error contains considerably fewer terms and the corresponding coefficients for each term are given in Tables 5–7. These tables give the errors in the machine coordinate system $O4$ fixed to the machine frame.

Table 7
Orientation error dk in machine coordinates

Error dk in machine coordinates	Coefficient
First order error is zero	0

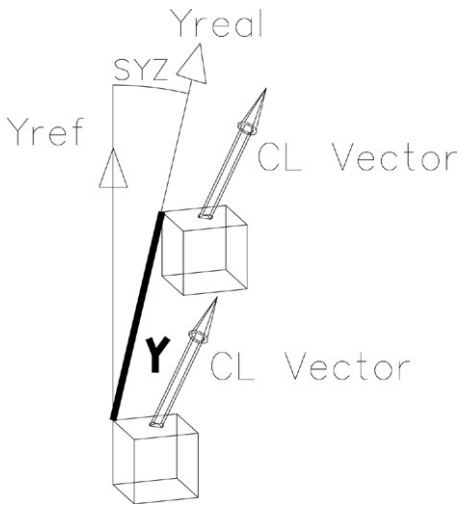

Fig. 6. Effect of S_{YZ} on CL vector orientation.

It can be observed that the error components S_{YZ}, R_{BZ}, R_{XZ}, R_{YZ} and R_{ZZ} do not affect the first order angular errors. This is as expected. An upward slide motion along the real Y-axis will not introduce an error in the orientation when the workpiece moves along the real Y-axis as shown in Fig. 6.

All the rotational errors of the X, Y, Z and B-body (R_{XZ}, R_{YZ}, R_{ZZ}, R_{BZ}) around the Z-axis also have no first order influence. This can also be explained by the fact that the tool is always along the Z-axis and the difference between the transformed CL vector orientation is only di and dj. So small rotations around the Z-axis will have only a second order effect for the specific machine under consideration (Fig. 1). The rotation of the A body around the Z-axis however has and effect that varies with the position (sin B) of the B-axis. When B is zero in the reference position the effect of R_{AZ} is null. The effect is maximum when B is 90°.

The error equations for the rotations have fewer terms because they are not affected by the translation errors. It is thus simple to identify these error components first and use the results later to identify the translational errors.

3.7. Observations concerning mathematical model

The equations giving the relations between the orientation errors contain only squareness errors and angular errors of the 5 rigid bodies. This means that the identification problem can be separated into two independent problems. A large part of the orientation errors can be identified independently by using the equations in Tables 5–7. Using the system of equations in the Tables 2–4 can identify the remaining orientation errors and translational errors.

The errors are approximated as one-dimensional polynomials of the main translation X, Y, Z or rotations A and B. So for example $R_{AX} = f(A)$, $R_{AY} = f(A)$, $R_{AZ} = f(A)$ or in general with our notation $R_{MX} = f(M)$, $R_{MY} = f(M)\ldots$.

Table 8
Maho 600E workspace in machine coordinates

Coordinate	Min value	Max value
$X1$	0 mm	300 mm
$Y1$	−150 mm	+150 mm
$Z1$	−150 mm	+150 mm
$I1$	0	+1
$J1$	−1	+1
$K1$	−1	+1

Table 9
Maho 600E 5-axis machine axis range for workspace in Table 8

Translation/rotation	Min value	Max value
X	−124 mm	266 mm
Y	−206 mm	187 mm
Z	−391 mm	1 mm
A	0°	360°
B	−180°	0°

The selection of an appropriate degree is often not an easy problem. The higher the degree the better the approximation. This can clearly be demonstrated by the expansion of a function in a Taylor series. However it is well known that in the numerical computations this can result in badly conditioned systems of linear equations.

Another problem is the fact that the cumulative systematic errors are the sum of the components contributed by each rigid body. So the error in the orientation of the CL vector di, dj and dk is the sum of a set of polynomials in the machine coordinates X, Y, Z, A and B. The linear equations obtained to identify the coefficients of the polynomials must be linear independent. The $\text{error}(X) = a_0 + a_1X + a_2X^2 + \cdots + a_nX^n$ for different sampled locations $X = X1, X2\ldots$ will be linear independent equations. However the equation obtained in the model is the sum of polynomials in the different machine coordinates as follows.

$\text{Error}(X, Y, Z, A, B) = a_0 + a_1X + a_2X^2 + \cdots + a_nX^n + b_0 + b_1Y + b_2Y^2 + \cdots + b_nY^n + \cdots + e_0 + e_1B + e_2B^2 + \cdots + e_nB^n$. The $a_i, b_i, \ldots, e_i$, can be any T_{MN} or R_{MN} depending on the case.

To obtain linear independent equations for different machine coordinates we must use sets of linear independent machine coordinates so each of the coordinates sets $\{X, Y, Z, A, B\}$ must be linear independent.

4. Solution of the mathematical model

4.1. Workspace of the 5-axis machine tool

It is important to identify the systematic errors in the whole workspace of the machine tool. In the case considered here the workspace in the workpiece coordinate system is given in Table 8. This is based on the size of the machine table.

The corresponding machine translations and rotations X, Y, Z, A, B is given in Table 9. The real travel ranges of the Maho 600E machine are as follows:

Table 10
Scaling of the machine range for polynomials

Scaling function	Min	Max
$Xp = (X - X_{\min})/(X_{\max} - X_{\min})$	0	1
$Yp = (Y - Y_{\min})/(Y_{\max} - Y_{\min})$	0	1
$Zp = (Z - Z_{\min})/(Z_{\max} - Z_{\min})$	0	1
$Ap = (A - A_{\min})/(A_{\max} - A_{\min})$	0	1
$Bp = (B - B_{\min})/(B_{\max} - B_{\min})$	0	1

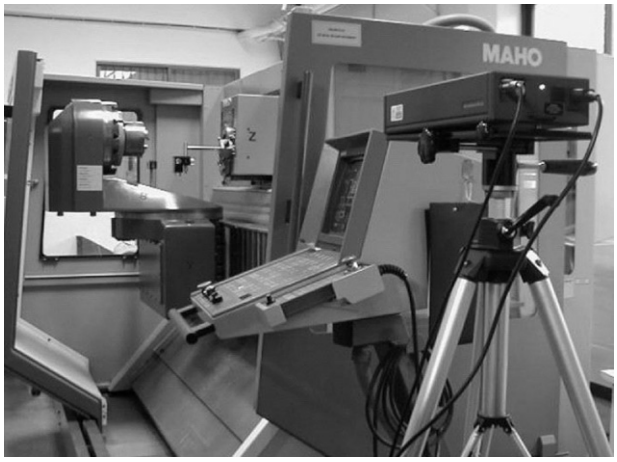

Fig. 7. Direct measurement with interferometer.

X range = 600 mm, Y range = 450 mm, Z range = 400 mm, A range 360°, B range 15° to −195° (for references as in Fig. 1). The CNC controller is Phillips 432 5-axis simultaneous. As can be seen from the Table 9, we cover practically the whole range of machine slide travel in our model.

The ranges in Table 9 will be used to scale the range of the independent variables of the polynomial approximation. The range will be scaled to vary from 0 to 1. The scaling of the independent variables based on Table 9 gives Table 10.

This scaling reduces the numerical instability (condition number) of the computation.

4.2. Simulation

4.2.1. Simulated error data

To study the numerical behavior of the model simulated errors are used. Based on the literature survey it looks acceptable to use cubic polynomials for the rotational and translational systematic errors. The squareness errors are constant small angles. Also the linear position errors were measured with the interferometer as shown in Fig. 7. The averaged results for the X, Y and Z axis are shown in Fig. 8. From these it also looks acceptable to use cubic polynomials.

A cubic polynomial with its maximum, minimum and inflexion point in the range $0 < X < 1$ is $(100X^3 - 140X^2 + 53X - 4)$. In the simulation this basic polynomial is multiplied by a scaling factor to obtain small rotational and translational error components.

For the rotational errors the scaling factor used is 10^{-4}, for the translational errors 10^{-3}.

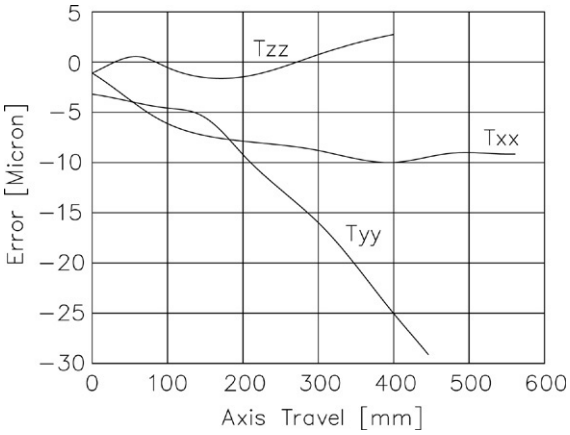

Fig. 8. Maho 600E error T_{XX}, T_{YY}, T_{ZZ} obtained by interferometer.

The absolute values of these simulated errors correspond to values found in accurate machine tools.

For all the squareness errors ($S_{AX} \ldots S_{ZY}$) in the simulation the same constant value of 0.00001 rad is used.

All rotational errors in radians will have the form:

$$R_{MN}(M) = R_{MN3}M^3 + R_{MN2}M^2 + R_{MN1}M + R_{MN0}.$$

The translational errors in mm will have the form:

$$T_{MN}(M) = T_{MN3}M^3 + T_{MN2}M^2 + T_{MN1}M + T_{MN0}.$$

Parameter M has the value ranges given in Table 10. With these polynomials the simulated errors $\mathrm{d}X$, $\mathrm{d}Y$, $\mathrm{d}Z$ and $\mathrm{d}i$, $\mathrm{d}j$ can be computed with the equations in Tables 2–7.

4.2.2. Identification of the orientation errors

The coefficient matrix of the linear system to identify the rotational or orientations errors can be obtained from Tables 5–7. The total number of unknown are the 9 rotational error components R_{AY}, R_{BY}, R_{XY}, R_{YY}, R_{ZY}, R_{BX}, R_{XX}, R_{YX}, R_{ZX} and the 6 squareness errors S_{AY}, S_{AZ}, S_{ZY}, S_{ZX}, S_{BX}, S_{BZ}. Two independent systems of linear equations, one for $\mathrm{d}i$ and one for $\mathrm{d}j$, are obtained. The 8 error components R_{AY}, R_{BY}, R_{XY}, R_{YY}, R_{ZY} and S_{AY}, S_{AZ}, S_{ZY} only influence the X component $\mathrm{d}i$. This provides the first set of linear equations that can be solved separately. The 7 error components R_{BX}, R_{XX}, R_{YX}, R_{ZX} and S_{ZX}, S_{BX}, S_{BZ} only influence the Y component $\mathrm{d}j$. This will be the second set of linear equations that can be solved separately.

The rotational error components are approximated by cubic polynomials and the straightness errors by constants. So in the case of the first system of equations there are 23 ($5 \times 4 + 3$) unknown coefficients; in the case of the second system there are 19 ($4 \times 4 + 3$) unknowns. It should however be clear that it is not possible to separate the polynomials constant terms R_{MN0} from S_{MN}. Only the sum of constants ($R_{AY0} + R_{BY0} + R_{XY0} + R_{YY0} - R_{ZY0} - S_{ZY}$), and the constants S_{AY} and S_{AZ} can be identified from the first linear system.

Only the sum of constants ($R_{BX0} + R_{XX0} + R_{YX0} - R_{ZX0} - S_{ZX} + S_{BX}$), ($S_{BX} - R_{AX0}$) and ($S_{BZ} - R_{AZ0} - S_{AZ}$) can be identified from the second linear system. The total number of

Table 11
Coefficients identified from di

	Coefficient	Error component coefficient	Error (%)
1	1	$R_{AY0} + R_{BY0} + R_{XY0} + R_{YY0} - R_{ZY0} - S_{ZY} + S_{AY}$	−4.9
2	Ap^3	R_{AY3}	0.2
3	Ap^2	R_{AY2}	0.2
4	Ap	R_{AY1}	0.2
5	Bp^3	R_{BY3}	0.09
6	Bp^2	R_{BY2}	0.05
7	Bp	R_{BY1}	−0.01
8	Xp^3	R_{XY3}	0.10
9	Xp^2	R_{XY2}	0.10
10	Xp	R_{XY1}	0.12
11	Yp^3	R_{YY3}	0.14
12	Yp^2	R_{YY2}	0.15
13	Yp	R_{YY1}	0.15
14	Zp^3	R_{ZY3}	−0.01
15	Zp^2	R_{ZY2}	−0.01
16	Zp	R_{ZY1}	−0.01
17	$-\cos[A]$	S_{AY}	0.65
18	$\sin[A]$	S_{AZ}	−0.1

Table 12
Coefficients identified from dj

	Coefficient	Error component coefficient	Error (%)
1	1	$R_{BX0} - R_{XX0} - R_{YX0} + R_{ZX0} - S_{BX} + S_{ZX}$	0.125
2	Bp^3	R_{BX3}	0.3
3	Bp^2	R_{BX2}	−0.71
4	Bp	R_{BX1}	−3.77
5	Xp^3	R_{XX3}	−0.1
6	Xp^2	R_{XX2}	0
7	Xp	R_{XX1}	0
8	Yp^3	R_{YX3}	−0.1
9	Yp^2	R_{YX2}	0
10	Yp	R_{YX1}	−0.19
11	Zp^3	R_{ZX3}	0
12	Zp^2	R_{ZX2}	0
13	Zp	R_{ZX1}	0
14	$\cos[B]$	$-R_{AX0} + S_{BX}$	−0.4
15	Ap^3	R_{AX3}	−0.3
16	Ap^2	R_{AX2}	−0.71
17	Ap	R_{AX1}	−0.38
18	$\sin[B]$	$-R_{AZ0} - S_{AZ} + S_{BX}$	−3
19	$Ap^3 \sin[B]$	R_{AZ3}	−0.2
20	$Ap^2 \sin[B]$	R_{AZ2}	0
21	$Ap \sin[B]$	R_{AZ1}	−0.19

unknown is thus reduced to 18 for the first system and 21 for the second. Solution of these two systems of equation by the least squares methods gives the results summarized in Tables 11 and 12. The least square approach now finds without any problem the solution to this reduced linear system.

The condition number for the first system is 1304.85 and for the second system 71,403.9. The residual error is between 10^{-8} and 10^{-9} for both systems or three orders of magnitude smaller than the values of di and dj, and thus very acceptable.

Table 13
The error terms and coefficients of dX in workpiece coordinates

	Error component	Coefficient
1	$T_{BX} + T_{XX} + T_{YX} - T_{ZX}$	1
2	$R_{BZ} + R_{XZ} + R_{YZ} + S_{BZ} - S_{YZ}$	Y
3	T_{AX}	$\cos[B]$
4	T_{AZ}	$\sin[B]$

The last column in Tables 11 and 12 gives the error between the estimated value with the first order model and the real values.

The parameters that influence the orientation errors have now been identified. At this stage all the error components that influence the angular errors have been identified for the simulation. A total of minimum 21 CL vectors is required to identify the rotational components.

If the linear accuracy of the machine is considered sufficient there is no more need to compensate the linear errors. The compensation proposed in Section 5.1 can be applied after identification. Only implementation of this step could improve considerably the accuracy of swarf milling of ruled surfaces where the cutter contact is not a point but a curve [31].

4.2.3. *Simulated identification of the translation errors*

The linear error can now be identified based on the equations in Tables 2–4. The orientation errors identified above can be substituted in these equations thus reducing the size of the systems of linear equations considerably. This will also give better numerical stability and smaller condition numbers.

4.2.3.1. Identification of the dX *translation errors.* Table 13 gives the error terms that affect dX without the known angular terms.

To find the coefficients of the polynomial approximation of the error terms, the constant terms and the polynomial coefficients that are linear dependent must be combined. For example the coefficient $T_{YX3}\ Yp^3$ will be linear dependent with $R_{YZ2}\ yp^2\ Y$. So only the sum of the two coefficient can be computed. Another approach is to vary only a certain number of machine coordinates X, Y, Z, A, B stepwise. By keeping the Y and the B machine coordinate zero while randomly changing the other machine coordinates X, Z, A, a smaller system of linear equations can be obtained, and no linear dependent polynomial terms except the constants. The non-zero terms are given in Table 14 including the estimation error in the value of the parameter in per cent.

The condition number of the matrix is 238.589. The value in Table 14 of $Yp = 0.33$ corresponds to a $Y = 0$ machine translation. In the next step the machine coordinate A is kept zero and the other machine coordinates X, Y, Z and B are randomly varied in the machine workspace. The set of coefficients that can now be determined is given in the Table 15.

The condition number is 116,000. The residuals are between 10^{-4} and 10^{-5}.

The coefficients T_{AZ3}, T_{AZ2} and T_{AZ1} must still be identified. This can be done by keeping Xp, Yp, Zp all zero, $Bp = 1$ and only varying A. The results are given in Table 16.

Table 14
Coefficients identified from dX by varying X, Z and A machine coordinates

	Coefficient	Error component coefficient	Error (%)
1	1	$T_{BX0}+T_{XX0}+T_{YX3}\,Yp^3+T_{YX2}\,Yp^2+T_{YX1}\,Yp+T_{YX0}-T_{ZX0}$	−45.8
2	Xp^3	T_{XX3}	15.72
3	Xp^2	T_{XX2}	25.43
4	Xp	T_{XX1}	40
5	$-Zp^3$	T_{ZX3}	0.59
6	$-Zp^2$	T_{ZX2}	−6.57
7	$-Zp$	T_{ZX1}	−16.1
8	$Ap^3\cos[B]$	T_{AX3}	−70.2
9	$Ap^2\cos[B]$	T_{AX2}	−56.6
10	$Ap\cos[B]$	T_{AX1}	−30.9
11	$\cos[B]$	T_{AX0}	80.75

Table 15
Coefficients identified from dX by varying X, Y, Z, B and $A=0$

	Coefficient	Error component coefficient	Error (%)
1	Bp^3	$T_{BX3}+Y_{\min}R\;R_{BZ3}$	1.37
2	Bp^2	$T_{BX2}+Y_{\min}R\;R_{BZ2}$	−6.63
3	Bp	$T_{BX1}+Y_{\min}R\;R_{BZ1}$	−38.6
4	1	$T_{BX0}+T_{XX0}+T_{YX0}-T_{ZX0}+Y_{\min}R(R_{BZ0}+R_{XZ0}+R_{YZ0}+S_{YZ})$	−19.6
5	Yp^4	$R_{YZ3}(Y_{\max}R-Y_{\min}R)$	−3.79
6	Yp^3	$(R_{YZ3}Y_{\min}R+R_{YZ2}(Y_{\max}R-Y_{\min}R)+T_{YX3})$	−4.26
7	Yp^2	$(R_{YZ2}\,Y_{\min}R+R_{YZ1}(Y_{\max}R-Y_{\min}R)+T_{YX2})$	−4.77
8	Yp	$(R_{YZ1}\,Y_{\min}R+T_{YX1}+(Y_{\max}R-Y_{\min}R)(R_{BZ0}+R_{XZ0}+R_{YZ0}+S_{YZ}))$	−16.3
9	$(Y_{\max}R-Y_{\min}R)YpBp^3$	R_{BZ3}	−1.8
10	$(Y_{\max}R-Y_{\min}R)YpBp^2$	R_{BZ2}	−2.14
11	$(Y_{\max}R-Y_{\min}R)YpBp$	R_{BZ1}	−2.26
12	${}_{YX}p^3$	R_{XZ3}	−0.5
13	${}_{YX}p^2$	R_{XZ2}	−0.71
14	${}_{YX}p$	R_{XZ1}	−1.13
15	$\sin[B]$	T_{AZ0}	51.0

Table 16
Coefficients identified from dX by varying A only; Xp, Yp, Zp are all zero and $Bp=1$

	Coefficient	Error component coefficient	Error (%)
1	1	$T_{BX3}+Y_{\min}R\;R_{BZ3}+T_{BX2}+Y_{\min}R\;R_{BZ2}+T_{BX1}+Y_{\min}R\;R_{BZ}1+T_{AZ0}+T_{BX0}+T_{XX0}+T_{YX0}-T_{ZX0}+Y_{\min}R(R_{BZ0}+R_{XZ0}+R_{YZ0}+S_{YZ})$	−24.2
2	$Ap^3\sin[B]$	T_{AZ3}	28.2
3	$Ap^2\sin[B]$	T_{AZ2}	23.6
4	$Ap\sin[B]$	T_{AZ1}	31.5

The condition number is 110 and all the residuals are less then 10^{-6}.

Table 17
The error terms and coefficients of dY in workpiece coordinates

Error component	Coefficient
$T_{AY}+T_{BY}+T_{XY}+T_{YY}-T_{ZY}$	1
$R_{BZ0}+R_{XZ0}+S_{BZ}$	$-X$

Table 18
The error terms and coefficients of dZ in workpiece coordinates

Error component	Coefficient
$T_{BZ}+T_{XZ}+T_{YZ}-T_{ZZ}$	1
$R_{AY0}+R_{BY0}+R_{XY0}$	X

T_{BX3}, T_{BX2}, T_{BX1} can be solved separately from the equations in the rows 1, 2, 3 and rows 9, 10, 11 in Table 15.

The individual coefficients T_{YX3}, T_{YX2}, T_{YX1}, R_{YZ3}, R_{YZ2}, R_{YZ1} and the sums of constants $(R_{BZ0}+R_{XZ0}+R_{YZ0}+S_{YZ})$ and $(T_{BX0}+T_{XX0}+T_{YX0}-T_{ZX0})$ can be solved separately from the equations in row 1 in Table 14, and rows 4, 5, 6, 7, 8 in Table 15.

The errors in the estimation of the parameters is given in per cent in the last column of Tables 14–16. It can be observed that the estimation errors are larger than the estimation errors in the case of the orientation errors (Section 4.2.2). This is probably due to the larger number of parameters and the fact that the estimated results of the orientation errors are used. Another reason is that the highest degree terms in the translation errors are quartic due to the fact that the linear error due to the rotation errors are multiplied by the length. The more important residual errors are however very acceptable. Minimum 30 different CL vectors are needed to identify all the coefficients having an effect on dX.

4.2.3.2. Identification of the dY *and* dZ *translation errors.* All the terms in the relation dX are now identified. The same must be done for dY and dZ. Only the terms not identified above in dX must be identified. Tables 17 and 18 give the error components that still need to be identified based on dY and dZ errors. The method to compute these coefficients is exactly the same as for dX.

An additional 17 CL vectors are required to identify all the unknown coefficients influencing dY and 14 more for dZ.

5. Compensation

Both the angular and translatory systematic errors can be compensated by means of an additional very simple step in the post processor where the G-codes are adjusted with the corrections $\mathrm{d}A, \mathrm{d}B, \mathrm{d}X, \mathrm{d}Y$, and $\mathrm{d}Z$. The CNC control for the case study machine has for each controlled axis two compensation tables: one for the linear compensation and one for the cyclic compensation. For 25 equally spaced points over the axis range we can enter the compensation values. However as the total volumetric error at each point in the workspace is a function of all the axes positions it cannot be used here. The compensation through software was the only option here.

5.1. Compensation of the angular errors

Once the systematic error functions coefficients have been determined they should be used to compensate. The problem looks quite complex. However if the real values for A and B will only differ from the reference values Aref and Bref by small first order differences the total differential of Eq. (3) can be used. Therefore it is faster to compute the correction of the A and B angles based on the inverse kinematics relations between A and B and i, j, k without systematic errors based on the total differential of both of these relations. For the 5-axis machine tool considered here the relations are in matrix notation:

$$\begin{bmatrix} \mathrm{d}i \\ \mathrm{d}j \\ \mathrm{d}k \end{bmatrix} = \begin{bmatrix} 0 & -\cos B \\ \cos B \cos A & -\sin B \sin A \\ -\sin A \cos B & -\cos A \sin B \end{bmatrix} \begin{bmatrix} \mathrm{d}A \\ \mathrm{d}B \end{bmatrix}. \tag{8}$$

The inverse solution of this equation is used to find the corrections $\mathrm{d}A$ and $\mathrm{d}B$.

The correctness of this approach however is not always valid, as can be observed from the following example. Consider a nominal CL vector with components $X1, Y1, Z1$ any coordinate but $i = 1$ and $j = k = 0$. The real CL vector will contain small errors $\mathrm{d}i, \mathrm{d}j$ and $\mathrm{d}k$. The required A rotation to compensate these errors will be large and a first approximation can be computed with $A = \mathrm{arctg}[\mathrm{d}j/\mathrm{d}k]$ from Eq. (3). This new A rotations will generate new errors $\mathrm{d}i, \mathrm{d}j$ and $\mathrm{d}k$ not correlated with the ones for $A = 0$. Also there will be very different values for the corresponding machine translations, so no convergence for a combination of machine coordinates can be found. This is a clear proof that to compensate this case will require an additional rotary C-axis. Three rotational axes allow to compensate each angular error $\mathrm{d}i, \mathrm{d}j, \mathrm{d}k$ by small rotations $\mathrm{d}A, \mathrm{d}B, \mathrm{d}C$. The $\mathrm{d}k$ and $\mathrm{d}i$ errors can be compensated in this case but not the $\mathrm{d}j$. A numerical example is discussed in Section 6.

5.2. Compensation of the translatory errors

The computation of the compensations for the slide motions X, Y, Z are obtained by computing the total differential of Eq. (3) :

$$\begin{aligned}
\mathrm{d}X\mathrm{cor} &= -Zo2o3\cos[B]\mathrm{d}B - Z1\cos[A]\cos[B]\mathrm{d}B \\
&\quad - \cos[B]\mathrm{d}X1 - Y1\cos[B]\mathrm{d}B\sin[A] \\
&\quad - Y1\cos[A]\mathrm{d}A\sin[B] + X1\mathrm{d}B\sin[B] \\
&\quad - \cos[A]\mathrm{d}Z1\sin[B] + Z1\mathrm{d}A\sin[A]\sin[B] \\
&\quad - \mathrm{d}Y1\sin[A]\sin[B]; \\
\mathrm{d}Y\mathrm{cor} &= z1\cos[A]\mathrm{d}A - \cos[A]\mathrm{d}Y1 \\
&\quad + Y1\mathrm{d}A\sin[A] + \mathrm{d}Z1\sin[A]; \\
\mathrm{d}Z\mathrm{cor} &= Y1\cos[A]\cos[B]\mathrm{d}A - X1\cos[B]\mathrm{d}B \\
&\quad + \cos[A]\cos[B]\mathrm{d}Z1 - Z1\cos[B]\mathrm{d}A\sin[A] \\
&\quad + \cos[B]\mathrm{d}Y1\sin[A] - Zo2o3\mathrm{d}B\sin[B] \\
&\quad - Z1\cos[A]\mathrm{d}B\sin[B] - \mathrm{d}X1\sin[B] \\
&\quad - Y1\mathrm{d}B\sin[A]\sin[B].
\end{aligned} \tag{9}$$

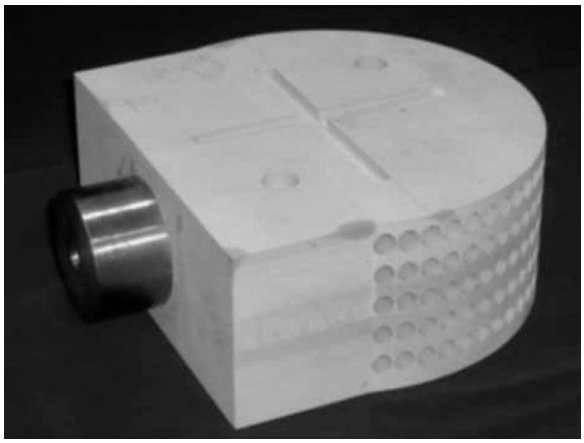

Fig. 9. Sample workpiece.

The computed errors $\mathrm{d}X\mathrm{cor}$, $\mathrm{d}Y\mathrm{cor}$, $\mathrm{d}Z\mathrm{cor}$ are added to the slide motions X, Y, Z. In the case of $\mathrm{d}A$ large, as in Section 6, Eq. (3) must be used to compute the new values of the corrected machine translations.

6. Implementation and experiments

The model to identify the parameters has now been built and analyzed based on simulated errors. The results show very clearly that all relevant coefficients can be identified without numerical problems, at least for cubic polynomials.

The input to the model is the CL vectors X, Y, Z, i, j, k that were generated with simulated errors. For example, in Table 15 the polynomial coefficients are identified based on CL points generated by motion along X, Y, Z and B machine axes while keeping A rotation zero (see Fig. 9).

The approach that was implemented was drilling holes in a sample workpiece and measuring the result on a CMM machine (Figs. 9 and 10). The advantages of this approach are many, such as:

(i) During drilling only one machine axis moves while all the other axes are positioned before the drilling starts.
(ii) If the depth of the hole is relatively short compared to the Z axis travel it is legitimate to assume that the Z body errors do not vary significantly over the length of the hole.
(iii) The downtime of the machine for the experiments is small.
(iv) Machine deformation can be minimized by slow feed.

The above method can be improved by drilling conical holes. This does not require that the Z body errors do not vary significantly over the length of the hole.

The Figs. 9 and 10 show one of the workpieces that were used to identify the closed loop error and the measurement on the CMM.

The difference in the location and orientation of the holes with the nominal position was measured and based on these values the parameters were identified.

The results were verified by drilling holes of diameter 10 mm in a square block 200 × 200 × 100 mm. The nominal CL vectors are given in Table 19. After drilling holes the exact

Fig. 10. Measurement on CMM machine.

Table 19
Nominal CL vectors in $O1$

$X1$	$Y1$	$Z1$	$i1$	$j1$	$k1$
100	−80	80	0.57735	−0.57735	0.57735
100	−80	−80	0.57735	−0.57735	−0.57735
100	80	−80	0.57735	0.57735	−0.57735
100	80	80	0.57735	0.57735	0.57735

Table 20
Measured real position of holes no compensation

$X1$	$Y1$	$Z1$	$i1$	$j1$	$k1$
100.169	−79.9989	79.82518	0.578441	−0.57753	0.576086
100.1571	−79.823	−80.0169	0.578352	−0.57607	−0.57763
100.1379	80.01842	−79.8447	0.578215	0.57764	−0.5762
100.1549	79.84416	79.99794	0.578338	0.576192	0.577522

Table 21
Measured real position of holes after compensation

$X1$	$Y1$	$Z1$	$i1$	$j1$	$k1$
100.001	−80.002	80.009	0.577351	−0.57735	0.577353
100.001	−80.001	−80.002	0.577351	−0.57735	−0.57735
100.002	80.006	−80.000	0.577351	0.577351	−0.57735
100.001	80.005	80.004	0.57735	0.577351	0.577353

Table 22
Nominal CL vectors in $O1$

$X1$	$Y1$	$Z1$	$i1$	$j1$	$k1$
−150.314	−80	80	1	0	0

locations and orientations were measured on a CMM machine. The measured results are given in Table 20. The holes drilled with the compensated G-codes were also measured with the CMM and Table 21 shows the considerable improvement.

Table 23
Measured real position of holes on CMM without compensation

$X1$	$Y1$	$Z1$	$i1$	$j1$	$k1$
−150.253	−80.048	80.052	1.00000	−0.00016	−0.00116

Table 24
Measured real position of holes with compensation with Eq. (9)

$X1$	$Y1$	$Z1$	$i1$	$j1$	$k1$
−150.318	−80.672	80.796	1.00000	−0.000147	0.0000505

Table 25
Measured real position of holes compensation with Eq. (3)

$X1$	$Y1$	$Z1$	$i1$	$j1$	$k1$
−150.210	−80.078	80.089	1.00000	−0.000304	−0.00009

Table 26
Measured real position of holes with compensation but no dj compensation

$X1$	$Y1$	$Z1$	$i1$	$j1$	$k1$
−150.313	−80.000	−80.000	1.00000	−0.000160	−0.000001

The largest linear error in the hole position without compensation was 0.177 mm. With compensation the largest linear error became 0.009 mm, much closer to the machine resolution of 0.001 mm. The maximum orientation error was reduced from 0.058° to 0.0002° after compensation, lower then the angular resolution of 0.001°.

To complete the demonstration an example of partial compensation is discussed.

A hole is drilled with the CL vector nominally aligned with the X axis of the machine.

The results of the compensation attempts are given in Tables 22 and 23.

The required A rotation to compensate the measured dj and dk is large: 7.86°.

Drilling the hole with the "compensated" G-code gives no improvement in the dj component. The results for the X and Y locations is also completely wrong because Eq. (9) were used (Tables 24–26).

When the compensated machine rotation A is computed with Eq. (3), dB with Eq. (8), the new nominal X, Y, Z with Eq. (3) and the linear corrections corresponding to this new nominal values with Eq. (9), a new compensated G-code is obtained. This G-code will compensate X, Y, Z and di, dk but not dj. To avoid this swapping between the Eq. (3) and the differential Eqs. (8) and (9) it is faster to keep A zero and compensate the rest of the nominal G-code with the differentials obtained from (8) and (9). This leaves dj also uncompensated.

If the dj error is not acceptable, complete compensation can still be obtained by changing the initial set up in such a way that

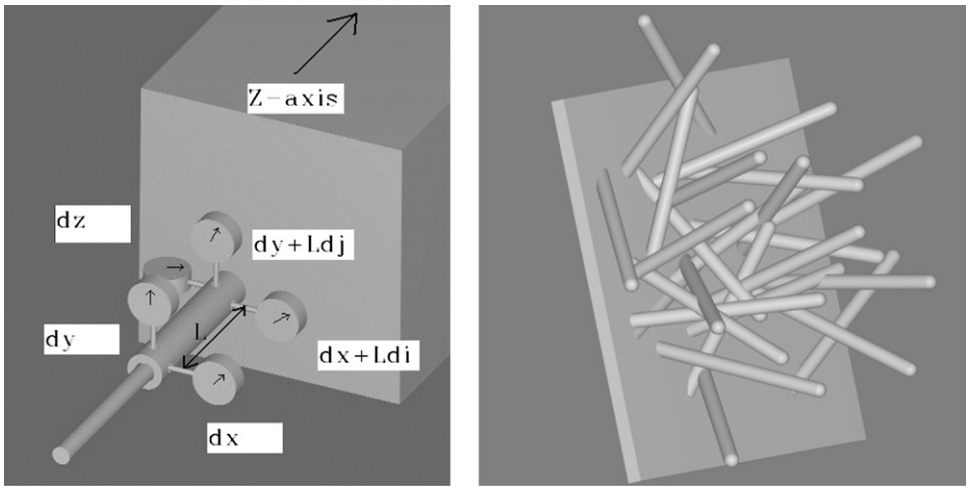

Fig. 11. Direct measurement of volumetric error with reference sleeve, dial indicator and cylinder tree.

none of the CL vectors have an orientation along the X-axis of the machine. A finite offset angle rotation around the Z axis would solve the problem by making the j component finite and not infinitesimal.

The above method can be further improved in accuracy by drilling the holes first and calibrating the holes on the CMM. The initial CNC program that was used to drill the holes is now adjusted based on the calibration results of the holes. The artifact is put on the machine again and the location is measured with measuring probe placed in the machine spindle. This method improves the accuracy but increases the time and cost.

7. Other compatible data sampling methods

Finally some new sampling methods that are compatible with the hole drilling approach are given below but were not implemented, for some of these the practical feasibility has to be investigated further.

- The real locations (CL points) could be generated by putting a reference cylinder in the spindle and measuring the real location relative to a coordinate system fixed to the machine table (workpiece coordinate system $O1$ in Fig. 1). This solution is however difficult to implement for the machine in Fig. 1. High resolution vision systems in the future could solve the problem.
- A hollow reference cylinder is placed in the spindle nose aligned precisely along the machine spindle centerline. The internal hole is about 1 mm larger than the reference cylinder diameter which is exactly known. A set of these reference cylinders is fixed to the machine table and the X, Y, Z, i, j, k in the workpiece coordinate system are known with an accuracy an order of magnitude higher then machine geometric errors. The machine is then programmed to insert these reference cylinders in the hole. The accurately positioned dial indicators will then measure directly the total geometric errors (Fig. 11). For each required sample CL point a reference cylinder must be fixed to the machine table.
- An auto collimator in the spindle and a mirror array on the artifact replaces the holes or cylinders on the artifact. This method could accurately measure $\mathrm{d}X, \mathrm{d}Y, \mathrm{d}Z$ and $\mathrm{d}i, \mathrm{d}j$ values. The image should be obtained through a digital camera.
- Standard methods [28] and commercially available systems [32] exist to measure all the 6 error components of each individual slide for a 3-axis machine tool. The method proposed here only differs from the standard method in that it is proposed to put the interferometer in the spindle and to measure $\mathrm{d}X, \mathrm{d}Y, \mathrm{d}Z$ and $\mathrm{d}i, \mathrm{d}k$ for a cluster of corner cubes and twin reflectors at each required CL point. This considerably reduces the number of measurement as the measurements are for the whole machine in one set up. A further benefit is that it is not necessary to measure the $\mathrm{d}k$ component. A CNC program is written to position the corner cubes and twin reflectors one by one consecutively in line with the interferometer axis at a constant nominal distance. The interferometer will measure $\mathrm{d}X, \mathrm{d}Y, \mathrm{d}Z$ and $\mathrm{d}i, \mathrm{d}j$ directly.

8. Conclusion

A new method to identify and compensate the systematic errors in a multi-axis machine tool has been presented. The mathematical model is based on a first order rigid body model of the machine tool. The angular errors can be identified independently of the translatory errors. The errors have been approximated by cubic polynomials in the monomial basis. The methodology to avoid numerical problems has been developed based on careful elimination of linear dependencies and breaking the large systems of linear equations in smaller ones. The angular errors are reduced from the theoretical number of 22 ($15R_{MN} + 7S_{MN}$) to only 13 ($11R_{MN}$ and S_{AY} and S_{AZ}). The other R_{MN} have no first order effect. The other S_{MN} are absorbed in the constant term of the polynomials. The translational errors are reduced from all 39 ($15T_{MN}$, $15R_{MN}$, $7S_{MN}$ and $2r_{AB}$) to only 19 ($15T_{MN}$, R_{BZ}, R_{XZ}, R_{YZ} and Z_{AB}). This is because the components

identified from the angular errors identification step are known already. The method has been investigated first with simulated errors. An implementation based on drilling holes in an artifact and measure the errors on a CMM machine was proposed. Finally new ways to measure the volumetric error directly were outlined. Direct measurement of the total volumetric error requires considerably less measurement then measuring all the 6 components of each machine slide, especially in case of a 5-axis machine. The proposed method can be extended to include the systematic error change due to the thermal and elastic deformation as variations of the identified error components as a function of the cutting force and temperature as suggested in [7,8].

References

[1] Bohez ELJ. Compensating for systematic errors in 5-axis NC machining. Computer-Aided Design 2002;34:391–403.

[2] Belforte G, Bona B, Canuto E, Donati F, Ferraris F, Gorini I, et al. Coordinate measuring machines and machine tools selfcalibration and error correction. Annals of the CIRP 1987;36(1):359–64.

[3] Kirienda VSB, Ferreira PM. Kinematic modeling of quasistatic errors of three-axis machining centers. International Journal of Machine Tools & Manufacture 1994;34(1):85–100.

[4] Kirienda VSB, Ferreira PM. Parameter estimation and model verification of first order quasistatic error model for three-axis machining centers. International Journal of Machine Tools & Manufacture 1994;34(1): 101–25.

[5] Kirienda VSB, Ferreira PM. Computational approaches to compensating quasistatic errors of three-axis machining centers. International Journal of Machine Tools & Manufacture 1994;34(1):127–45.

[6] Tajbakhsh H, Abain Z, Ferreira PM. $L\infty$ parameter estimates for volumetric error in models of machine tools. Precision Engineering 1997; 20:179–87.

[7] Soons JA, Theuws FC, Schellekens PH. Modeling the errors of multi-axis machines: A general methodology. Precision Engineering 1992;14:5–19.

[8] Srivastava AK, Veldhuis SC, Ebestawit MA. Modelling geometric and thermal errors in a five-axis CNC machine tool. International Journal of Machine Tools & Manufacture 1995;35(9):1321–37.

[9] Florussen GHJ, Delbressine FLM, van de Molengraft MJG, Schellekens PHJ. Assessing geometrical errors of multi-axis machines by three-dimensional length measurements. Measurement 2001; 30:241–55.

[10] Lin Y, Shen Y. Modelling of five-axis machine tool metrology models using the matrix summation approach. The International Journal of Advanced Manufacturing Technology 2003;21:243–8.

[11] Ramesh R, Mannan MA, Poo AN. Thermal error measurement and modelling in machine tools. Part I. Influence of varying operating conditions. International Journal of Machine Tools & Manufacture 2003; 43(4):391–404.

[12] Ramesh R, Mannan MA, Poo AN, Keerthi SS. Thermal error measurement and modelling in machine tools. Part II. Hybrid Bayesian Network-support vector machine model. International Journal of Machine Tools & Manufacture 2003;43(4):405–19.

[13] Bagshaw RW, Newman ST. Manufacturing data analysis of machine tool errors within a contemporary small manufacturing enterprise. International Journal of Machine Tools & Manufacture 2002;42:1065–80.

[14] Bjorklund S, Bjurstam P, Novak A. Compensation of systematic errors in five-axis high-speed machining. International Journal of Production Research 2002;40(15):3765–78.

[15] Wang S-M, Lui Y-L, Kang Y. An efficient error compensation system for CNC multi-axis machines. International Journal of Machine Tools & Manufacture 2002;42:1235–45.

[16] Jha BK, Kumar A. Analysis of geometric errors associated with five-axis machining centre in improving the quality of cam profile. International Journal of Machine Tools & Manufacture 2002;43:629–36.

[17] Lei WT, Hsu YY. Accuracy test of five-axis CNC machine tool with 3D probe-ball. Part I: Design and modeling; Part II: Errors estimation. International Journal of Machine Tools & Manufacture 2002;42:1153–62, 1163–70.

[18] Lei WT, Hsu YY. Accuracy enhancement of five-axis CNC machines through real-time error compensation. International Journal of Machine Tools & Manufacture 2003;43:871–7.

[19] Chen XB, Geddam A, Yuan ZJ. Accuracy improvement of three-axis CNC machining centers by quasi-static error compensation. Journal of Manufacturing Systems 1997;16(5).

[20] Mou J, Liu CR. A method for enhancing the accuracy of CNC machine tools for on-machine inspection. Journal of Manufacturing Systems 1992; 11(4):229–37.

[21] Mou J, Liu CR. A methodology for machine tools error correction using reference parts. International Journal of Computer Integrated Manufacturing 1995;8(1):64–77.

[22] Abbaszadeh-Mir Y, Mayer JRR, Cloutier G, Fortin C. Theory and simulation for the identification of the link geometric errors for a five-axis machine tool using a telescoping magnetic ball-bar. International Journal of Production Research 2002;40(18):4781–97.

[23] Mahbubur RMD, Heikkala J, Lappalainen K, Karjalainen JA. Positioning accuracy improvement in five-axis milling by post processing. International Journal of Machine Tools & Manufacture 1997;37(2): 223–36.

[24] Tsutsumi M, Saito A. Identification and compensation of systematic deviations particular to 5-axis machining centers. International Journal of Machine Tools & Manufacture 2003;43:771–80.

[25] Lee MC, Ferreira PM. Auto-triangulation and auto-trilateration. Part 1. Fundamentals. Precision Engineering 2002;26:237–49.

[26] Lee MC, Ferreira PM. Auto-triangulation and auto-trilateration. Part 2. Three-dimensional experimental verification. Precision Engineering 2002;26:250–62.

[27] Tutunea-Fatan OR, Feng H-Y. Configuration analysis of five-axis machine tools using a generic kinematic model. International Journal of Machine Tools & Manufacture 2004;44:1235–43.

[28] Weck M, Bibring H. Metrological analysis and performance tests. Handbook of machine tools, vol. 4. Wiley Heyden Ltd.; 1984.

[29] Kruth JP, Vanherck P, De Jonge L. Self-calibration method and software error correction for three-dimensional coordinate measuring machines using artefact measurement. Measurement 1994;14:157–67.

[30] Goldstein H. Classical mechanics. 2nd ed. Addison-Wesley Publishing Company; 1980.

[31] Bohez ELJ, Senadhera SDR, Pole K, Duflou JR, Tar T. A geometric modeling and 5-axis machining algorithm for centrifugal impellers. Journal of Manufacturing Systems 1997;16(6).

[32] Automatic Precision, Inc., API 6D Laser, www.apisensor.com.

Erik L.J. Bohez has been an Associate Professor in Design and Manufacturing at the Asian Institute of Technology, Thailand since 1985. He is teaching courses of Advanced Manufacturing Processes, CAD/CAM, FMS, Multi-Axis Machine Tools, Eco-Design and Manufacturing Systems. From 1980–1983 he was a professor in the Ecole Nationale d'Ingenieur, Bamako, Mali. He has 26 years' experience in industry and the academic world. He is a graduate of the State University of Ghent in Belgium. His research interests include Hyper-Redundant Bio-Inspired Robots, Modeling of FMS by PetriNet, Simulation of Metal Removal Processes, Robust Control, 5-axis Machining, Adaptive Control, CNC, Packaging Technology, and Biomedical Engineering. He has been a consultant to UNIDO, UNESCO and other international organizations. His e-mail address is: bohez@ait.ac.th.

Bancha Ariyajunya is a Lecturer in the Department of Industrial Engineering at Burapha University, Thailand. He received his undergraduate degree from Burapha University, Thailand, and his Master of Engineering from the Asian Institute of Technology, Thailand. His current research interests include CAD/CAM/CNC, geometric modeling and 5-axis machining.

Chanin Sinlapeecheewa graduated with a Bachelor degree in Mechanical Engineering from Kasetsart University, a Master degree in Manufacturing System Engineering from the Asian Institute of Technology and a Ph.D. from The University of Tokyo in 2004. His research interests include systematic error compensation, unconventional machining, reverse engineering and fast 3D profile measurement. After graduation, he joined Fabrinet Co., Ltd. as a senior engineer. His main responsibilities are process design and manufacturing of optical communication devices.

Tin Maung Maung Shein graduated with a Bachelor of Engineering degree in Mechanical Engineering from Yangon Technological University (formerly known as Yangon Institute of Technology), Myanmar in 1998 and a Master of Engineering degree in Industrial Engineering from the Asian Institute of Technology, Thailand in 2001. He is currently working as a Laboratory Supervisor in Industrial Systems Engineering, School of Engineering and Technology, Asian Institute of Technology. His research interests are Multi-axis CNC machining, CAD/CAM, Tooling & Instrumentation, Industrial Optimization and Quality Control & Management.

Do Tien Lap has been a lecturer at Le Qui Don Technical University, Hanoi, Vietnam for 6 years. He graduated from Le Qui Don Technical University with a degree of Engineer of machine manufacturing technology in 2000 and obtained a Master of Engineering Degree in Manufacturing Systems Engineering, Design and Manufacturing engineering from the Asian Institute of Technology in 2003. His research interests are Numerical Control, New Product Development, CNC machine and Technology of manufacturing on CNC machine. Currently he is working as lecturer at Le Qui Don Technical University in Hanoi, Vietnam, and studying for a Ph.D. in Bauman Moscow State University.

Gustavo Belforte graduated in Electronic Engineering in 1974. In 1975 he joined Politecnico di Torino where he covered several positions until 1985, when he became Associate Professor of Automatic Control at Dipartimento di Automatica e Informatica. The research activity of Professor Belforte has been mainly focused on theoretic and applied problems related to modeling and identification of systems subject to bounded uncertainties. He also investigated classification and signal processing problems. In the early stage of its activity Professor Belforte was involved in biomedical applications, while in more recent years he worked on mechanical systems. He is author or co-author of more than hundred papers published in international journals, books and conferences. His e-mail address is: gustavo.belforte@polito.it.